The ribosomal protein S1-dependent standby site in *tisB* mRNA consists of a single-stranded region and a 5′ structure element

Cédric Romilly[a], Sebastian Deindl[b], and E. Gerhart H. Wagner[a,1]

[a]Department of Cell and Molecular Biology, Biomedical Center, Uppsala University, S-75124 Uppsala, Sweden; and [b]Department of Cell and Molecular Biology, Science for Life Laboratory, Uppsala University, 75124 Uppsala, Sweden

Edited by Gisela Storz, National Institute of Child Health and Human Development, Bethesda, MD, and approved June 25, 2019 (received for review March 12, 2019)

In bacteria, stable RNA structures that sequester ribosome-binding sites (RBS) impair translation initiation, and thus protein output. In some cases, ribosome standby can overcome inhibition by structure: 30S subunits bind sequence-nonspecifically to a single-stranded region and, on breathing of the inhibitory structure, relocate to the RBS for initiation. Standby can occur over long distances, as in the active, +42 *tisB* mRNA, encoding a toxin. This mRNA is translationally silenced by an antitoxin sRNA, IstR-1, that base pairs to the standby site. In *tisB* and other cases, a direct interaction between 30S subunits and a standby site has remained elusive. Based on fluorescence anisotropy experiments, ribosome toeprinting results, in vitro translation assays, and cross-linking–immunoprecipitation (CLIP) in vitro, carried out on standby-proficient and standby-deficient *tisB* mRNAs, we provide a thorough characterization of the *tisB* standby site. 30S subunits and ribosomal protein S1 alone display high-affinity binding to standby-competent fluorescein-labeled +42 mRNA, but not to mRNAs that lack functional standby sites. Ribosomal protein S1 is essential for standby, as 30ΔS1 subunits do not support standby-dependent toeprints and TisB translation in vitro. S1 alone- and 30S-CLIP followed by RNA-seq mapping shows that the functional *tisB* standby site consists of the expected single-stranded region, but surprisingly, also a 5′-end stem-loop structure. Removal of the latter by 5′-truncations, or disruption of the stem, abolishes 30S binding and standby activity. Based on the CLIP-read mapping, the long-distance standby effect in +42 *tisB* mRNA (∼100 nt) is tentatively explained by S1-dependent directional unfolding toward the downstream RBS.

translation initiation | ribosome standby site | RNA secondary structure | ribosomal protein S1 | fluorescence anisotropy

On many mRNAs, protein synthesis is limited by the rate of initiation (1). In bacteria, formation of the 30S preinitiation complex (30S-PIC) involves stochastic and reversible binding between the 30S ribosomal subunit, mRNA, and fMet-tRNA^{fMet}. Assisted by the initiation factors IF1, IF2, and IF3, the 30S becomes locked on the mRNA ribosome binding site (RBS), forming the 30S initiation complex (30S-IC) (2–7). In the canonical model, 2 RNA–RNA interactions are crucial for positioning and stabilization of this state. The Shine and Dalgarno (SD) sequence, upstream of the AUG start codon of the mRNA, base pairs with the anti-SD sequence near the 3′ end of 16S rRNA (8, 9), and the anticodon of fMet-tRNA^{fMet} base pairs with the start codon. Subsequent steps involve 50S joining, GTP hydrolysis on IF2, and dissociation of all IFs, whereupon the assembled 70S ribosome complex can enter elongation (10). Several studies have indicated that stable secondary structure at the RBS correlates with high translation efficiency (TE), whereas SD sequences appear to be less predictive of output (11–13).

Although stable RNA structure at an RBS is inhibitory for initiation (5, 14), some such mRNAs support surprisingly high translation rates (15–17). For example, a structured mRNA region can bind the so-called platform of the 30S subunit, using the SD/anti-SD interaction. Unfolding of the mRNA by ribosomal protein (r-protein) S1 promotes accommodation into the ribosome decoding channel (17, 18). A second strategy to overcome a stable, inhibitory structure at an RBS involves 30S subunit binding to a so-called ribosome standby site. This mechanism was first proposed to explain the high translation rate of the coat cistron of RNA phage MS2 (15, 19). Equilibrium models, taking the stability of the inhibitory RBS hairpin and the known 30S–mRNAs affinity into account, predicted coat translation rates 5 orders of magnitude lower than those empirically determined. To resolve this paradox, a model was proposed that involves sequence-nonspecific binding of a 30S subunit to a single-stranded segment of the mRNA (19). With a 30S ribosome on standby, initiation no longer depends on recruitment of the 30S subunit from the cytoplasm (second-order binding event), but instead on the unfolding/folding rates of the inhibitory hairpin (first order). Thus, a ribosome on standby competes efficiently with rapidly folding structures in an otherwise inaccessible RBS.

The standby model has since gained support outside the MS2 system. Biochemical experiments showed that 30S subunits bind a stable hairpin when preceded by a short tail of U-residues (20). We showed that short unstructured sequences preceding an inhibitory MS2 coat-like RBS hairpin can act as standby sites to

Significance

Ribosome standby is a mechanism that allows translation initiation at ribosome-binding sites that display stable, inhibitory structures. It involves initiator-tRNA-independent 30S subunit binding to single-stranded RNA regions, and the subsequent relocation to the sequestered ribosome-binding sites (RBS). Direct evidence for 30S preloading had previously been elusive. We report here on a detailed characterization of the standby site in *tisB* mRNA. 30S subunits bind to a single-stranded region and a 5′-stem-loop structure, as shown by fluorescence anisotropy experiments and footprint mapping by cross-linking–immunoprecipitation experiments. Ribosomal protein S1, on its own and in the context of the 30S ribosome, binds to the standby site. This is required for standby-dependent translation, likely reflecting S1-dependent directional unfolding over more than ≈100 nt to reach the sequestered RBS.

Author contributions: C.R., S.D., and E.G.H.W. designed research; C.R. performed research; C.R., S.D., and E.G.H.W. analyzed data; and C.R., S.D., and E.G.H.W. wrote the paper.

The authors declare no conflict of interest.

This article is a PNAS Direct Submission.

Data deposition: The raw sequencing data and processed results have been deposited on figshare (DOI: 10.6084/m9.figshare.8796698.v1).

[1]To whom correspondence may be addressed. Email: gerhart.wagner@icm.uu.se.

This article contains supporting information online at www.pnas.org/lookup/suppl/doi:10.1073/pnas.1904309116/-/DCSupplemental.

Published online July 18, 2019.

stimulate translation (21). Standby sites can also act at considerable distances from structured RBSs. The best-characterized naturally occurring system featuring a standby mechanism is the type I toxin/antitoxin locus *tisB/istR-1* in *Escherichia coli* (16, 22, 23). When induced by DNA damage, TisB depolarizes the inner membrane, induces growth arrest, and promotes persister cell formation (23, 24). In terms of mechanism, the primary *tisB* mRNA transcript (+1) is untranslatable because of structural inaccessibility of the *tisB* RBS. Upon processing, which removes the 5′-most 41 nt, the +42 mRNA becomes translatable, dependent on a structure change ~100 nt upstream of the RBS that exposes a single-stranded region as a standby site (16). The antisense sRNA IstR-1 inhibits TisB translation by preventing standby. This involves extensive, perfect base-pairing across the single-stranded segment (Fig. 1*A*) and RNA duplex cleavage by RNase III, generating the translationally inert +106 mRNA. That is, binding of 30S subunits to the standby site in +42 mRNA permits relocation to the sequestered *tisB* RBS upon breathing of this structure. In the absence of a standby site, as in the +1 and +106 variants, translation is inhibited (Fig. 1*A* and ref. 16).

There is strong circumstantial evidence for standby translation and its regulation by IstR-1. However, so far, no direct experimental evidence has shown a ribosome residing on a distal standby site. Here, we delineate the anatomy of the *tisB* mRNA standby site. Our results demonstrate $tRNA^{fMet}$-independent 30S subunit binding and an r-protein S1 requirement for standby. Cross-linking and immunoprecipitation (CLIP) experiments corroborate binding of S1 alone, as well as of 30S subunits, to the single-stranded standby region, and also to a short 5′ stem-loop structure. This structure is an unexpected element required for standby.

Results

$tRNA^{fMet}$-Independent 30S Subunit Binding to the +42 *tisB* mRNA Standby Site. Although previous data strongly support a standby mechanism, evidence for a direct 30S-standby site interaction on *tisB* mRNA had not been obtained. For instance, in the absence of $tRNA^{fMet}$, 30S toeprints were not seen near the standby sequence (16). We therefore measured direct binding of 30S subunits to the *tisB* standby site. Changes of fluorescence anisotropy of 3′-end FAM-labeled mRNAs were monitored in the presence of purified 30S subunits, as in ref. 25. Fluorescence anisotropy increased as a function of 30S concentration, indicating that the small subunit binds +42 *tisB* mRNA independently of $tRNA^{fMet}$ (apparent K_d, 26.9 ± 1.3 nM; Fig. 1*B*). This K_d value is consistent with known 30S affinities for mRNAs (19). To test whether binding occurred at the *tisB* standby site, 30S/+42 mRNA complex formation was challenged by the sRNA IstR-1, which base pairs at the standby sequence (16). IstR-1 dramatically reduced 30S binding to +42 *tisB* mRNA, making K_d value estimates unreliable (Fig. 1*B*). For further validation, 30S binding to 3′-end FAM-labeled +42 *tisB* mRNA was challenged by the addition of a 50-fold molar excess of unlabeled mRNA with (+42) or without (+106) a standby site (Fig. 1*A*). The presence of unlabeled +42 mRNA virtually abolished the 30S subunit-dependent increase in fluorescence anisotropy, indicating displacement of the FAM-labeled mRNA from the complex, whereas the +106 mRNA was inefficient as competitor (Fig. 1 *C* and *D*). These experiments suggest direct $tRNA^{fMet}$-independent 30S subunit binding to the +42 *tisB* standby site.

Ribosomal Protein S1 Is Essential for 30S Initiation Complex Formation on +42 *tisB* mRNA. We suspected that a protein component of the 30S subunit was, at least partially, responsible for standby binding. An obvious candidate is the r-protein S1 (26), as it is essential for ubiquitous translation in *E. coli* (27), binds single-stranded RNA (ssRNA) (28), binds to and accommodates structured mRNAs (17, 29), and can unwind RNA structure in vitro (30). To assess its requirement for *tisB* mRNA translation, 30S subunits were depleted of S1 (30SΔS1). As a control, toeprinting was carried out on *sodB* mRNA, the translation of which is S1-independent (17), which we confirmed here (*SI Appendix*, Fig. S2). In contrast, toeprints on +42 *tisB* mRNA were not observed in the absence of S1, but rescued upon its addition (Fig. 2*A*). The S1 requirement for standby-dependent translation was further assessed by in vitro

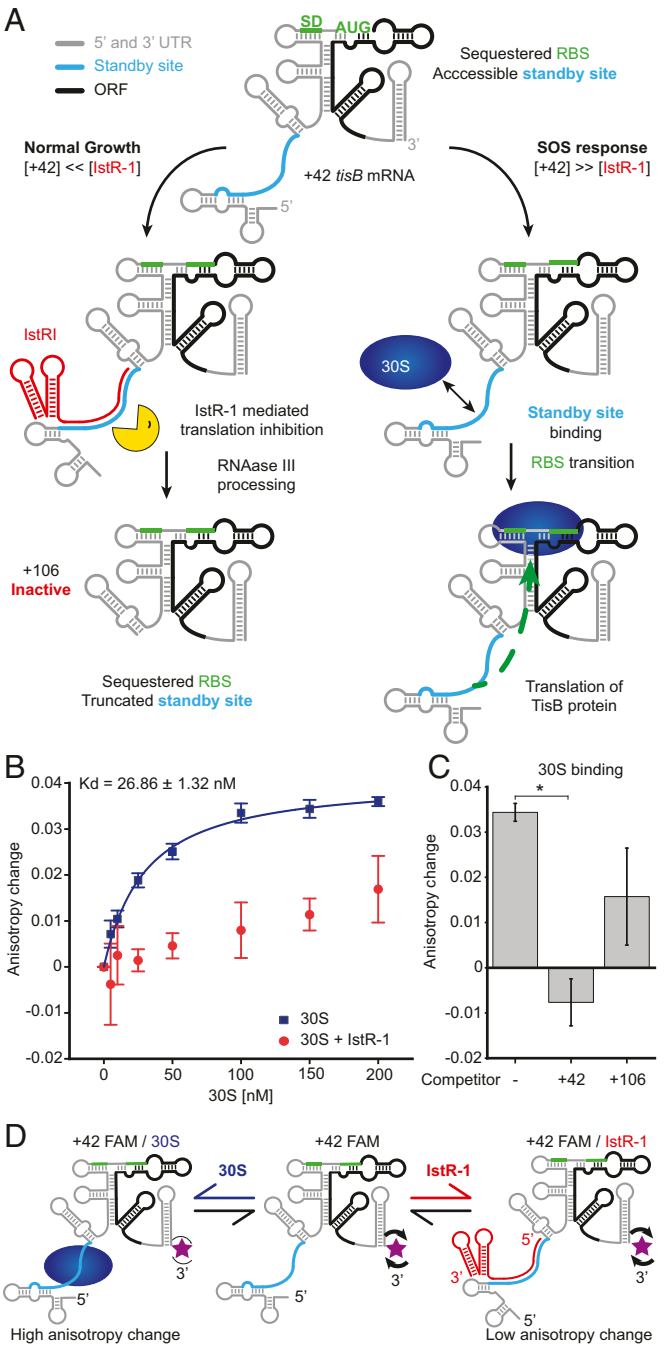

Fig. 1. $tRNA^{fMet}$-independent binding of 30S subunits to the *tisB* standby site. (*A*) Schematic secondary structure of the +42 mRNA: 5′ and 3′ UTR (gray), ORF (black), standby site (blue), SD, and AUG (green). Regulation is explained in the main text. (*B*) 5 nM of 3′-end FAM-labeled +42 *tisB* mRNA was incubated in the absence (blue squares) or presence of prebound IstR-1 (75 nM, red circles) at different concentration of 30S subunits. For information on experimental details and curve fitting, see *SI Appendix, SI Materials and Methods*. (*C*) 3′-end FAM-labeled +42 *tisB* mRNA (5 nM) incubated with 30S (150 nM), alone or with a 50-fold excess of unlabeled competitor (+42 or +106 mRNA). Anisotropy variation was calculated from 3 independent experiments. **T*-test *P* values < 0.05. (*D*) Schematics of effects on anisotropy of fluorescence emission on 30S or IstR-1 binding. Thin and thick arrows indicate low and high rotational diffusion, respectively. The purple star indicates the location of the 3′-end FAM dye.

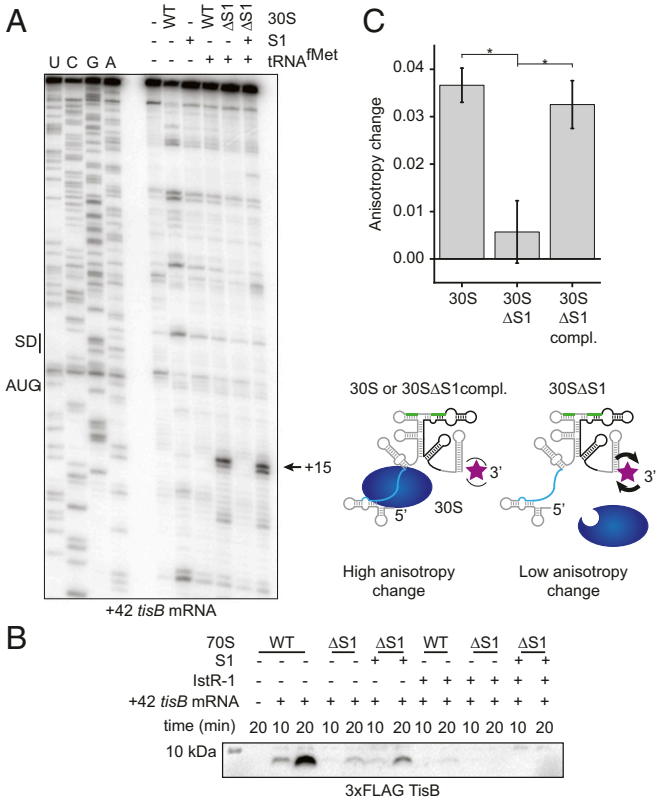

Fig. 2. Ribosomal protein S1 is required for *tisB* mRNA translation. (*A*) Toeprint assay on +42 *tisB* mRNA. Inclusion of 30S, 30S depleted of S1 (ΔS1), and 30SΔS1 complemented with a 3-fold excess of S1, is indicated, as is the presence of $tRNA^{fMet}$. Arrow: +15 relative to AUG. (*B*) In vitro translation of +42 *3xFLAG-tisB* mRNA, with 70S, 70S depleted of S1 (ΔS1), or 70SΔS1 complemented with 3-fold excess of S1. For controls, the presence of IstR-1 is indicated. TisB protein was detected by Western blot. (*C*) Fluorescence anisotropy variation of 3′-end FAM-labeled +42 mRNA (5 nM) with 30S, 30S depleted of S1 (30SΔS1), or 30SΔS1 complemented with S1 (all at 150 nM). **T*-test *P* values < 0.05. (*Bottom*) Schematic representation of competition effects on fluorescence anisotropy (see also Fig. 1*D*). The purple star indicates the location of the 3′-end FAM dye.

translation of a +42 *tisB-FLAG* mRNA. Inclusion of 70S ribosomes gave high levels of FLAG-tagged TisB, whereas 70SΔS1 ribosomes supported low levels, possibly because of residual S1 in the 30SΔS1 preparation (Fig. 2*B*). In line with the toeprint results, addition of S1 stimulated translation. As controls, IstR-1 completely inhibited all reactions (Fig. 2*B*). Hence, S1 is required for standby-dependent translation initiation (Fig. 2*A*) and overall translation of +42 *tisB* mRNA (Fig. 2*B*). Anisotropy experiments also showed that 30SΔS1 subunits exhibit substantially reduced binding to *tisB* mRNA, which was rescued by adding S1 in trans (Fig. 2*C*). We suggest that S1 anchors the 30S subunit to the *tisB* standby site.

30S Subunit, S1, and IstR-1 Binding Converges on the Standby Site. These experiments do not unambiguously imply direct binding of S1 to the standby site. Therefore, the affinity of S1 for *tisB* mRNA was first assessed by gel-shift. S1 bound tightly to radiolabeled +42 *tisB* mRNA with an apparent K_d of ∼25 nM (*SI Appendix*, Fig. S3). By fluorescence anisotropy, we therefore tested whether IstR-1 can block S1 binding to *tisB* mRNA. We used +42 mRNA FAM-labeled at the 5′-end, that is, near the standby site, to maximize the effect of S1 binding on rotational diffusion of the dye. Control experiments confirmed that 30S binding to 5′-end and 3′-end FAM-labeled mRNAs gave comparable K_d values (cf. Figs. 1*B* and 3*A*). Competition by unlabeled +42 mRNA was reproduced with the 5′-end FAM-labeled +42 mRNA, and unlabeled +106 mRNA was ineffective (Fig. 3*B*). As expected, IstR-1 inhibited 30S binding to the 5′-labeled mRNA (Fig. 3*B*), as it did on 3′-labeled mRNA (Fig. 1*B*).

Fig. 3*C* shows a near-stoichiometric S1 concentration-dependent binding curve. Clearly, S1 bound with high affinity to FAM-labeled *tisB* mRNA (apparent K_d value <10 mM; Fig. 3*C*), and IstR-1 decreased fluorescence anisotropy (Fig. 3*D*). This is expected from IstR-1-dependent sequestration of the standby site, which prevents access to S1 as well as 30S ribosomes. Competition assays added further corroboration. S1/+42 5′-end FAM-labeled mRNA complexes were challenged with an excess of unlabeled +42 or +106 mRNAs. Similar to the 30S results (Fig. 3*B*), +42 mRNA competed better than +106 mRNA for S1 binding (Fig. 3*D*). Raw data for 30S and S1 binding experiment are shown in *SI Appendix*, Fig. S4, and experiments to validate the specificity of interaction in *SI Appendix*, Fig. S1*A*.

Mapping of the S1/ 30S Subunit Binding Site by Cross-Linking. To precisely map 30S and S1 interactions with the +42 *tisB* mRNA, an in vitro CLIP approach was used. Briefly, the mRNA was incubated with substoichiometric concentrations of either purified 30S subunits (carrying S1-3xFLAG) or S1-3xFLAG only, followed by UV-cross-linking. 30S subunits, S1, and cross-linked RNAs were isolated by immunoprecipitation, followed by trimming of the bound RNA to generate footprints by deep RNA-seq (*SI Appendix*, *SI Materials and Methods*). Fig. 4*A* shows the footprint positions on the +42 *tisB* mRNA sequence (30S: ∼640,000 reads; S1: ∼1.1 million). Both 30S and S1 footprints mapped to the *tisB* mRNA standby site (position 85 to 111). Surprisingly, additional reads covered the far 5′ end of the mRNA (+42 to +69). Further cross-link reads were located in 2 structured regions of the mRNA, upstream of and within the *tisB* reading frame (Fig. 4), and are discussed in *Discussion*. The striking similarity between the S1 and 30S footprints suggests S1 to be the dominant contact with the mRNA. If other r-proteins had been efficiently cross-linked, this should have resulted in an enrichment in the

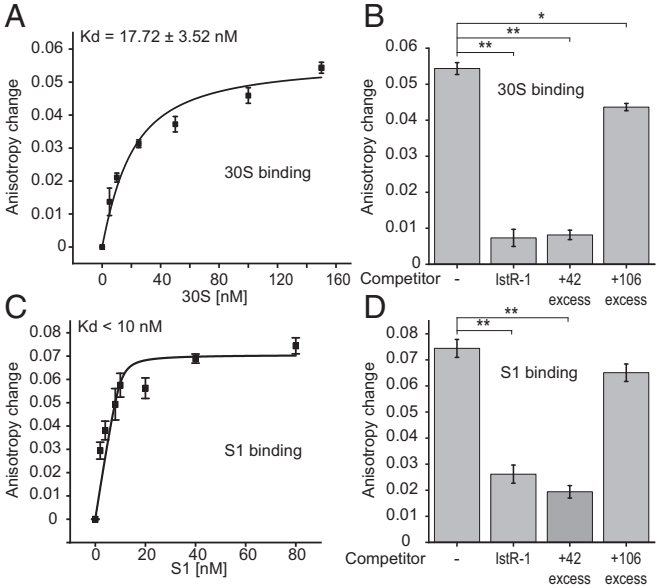

Fig. 3. Ribosomal protein S1 binds to the *tisB* mRNA standby site. 5′-end FAM-labeled +42 *tisB* mRNA (10 nM) was incubated with increasing concentrations of 30S subunits (*A*) or of protein S1 (*C*). Curve fitting was done as in Fig. 1. (*B*) Competition experiments with 5′-end FAM-labeled +42 *tisB* mRNA (10 nM). 30S subunits were at 150 nM, and additions of IstR-1 (200 nM) or competitor mRNAs (500 nM) are indicated. (*D*) As experiment in *B*, but with protein S1 (80 nM) instead of 30S subunits. Calculations are based on triplicates. **T*-test *P* value < 0.05; ***P* value < 0.005.

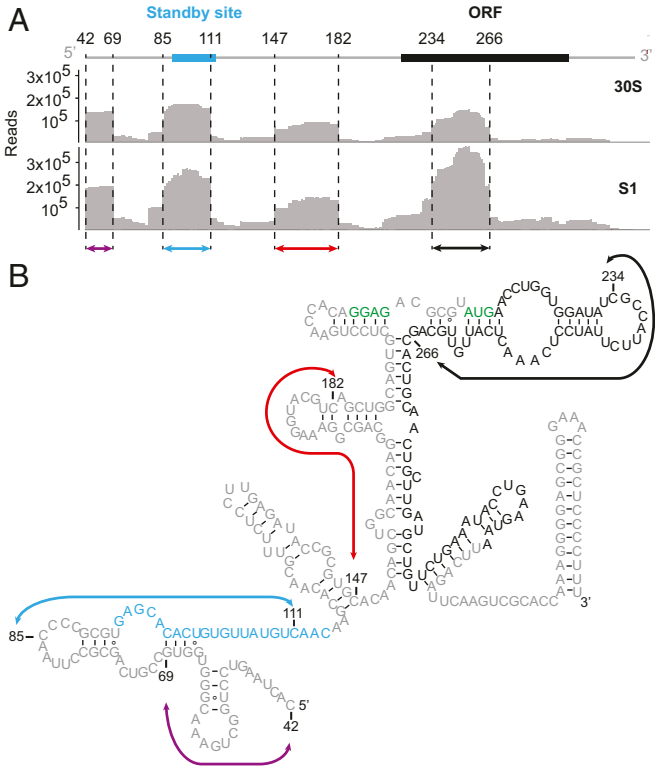

Fig. 4. Analysis of S1 and 30S binding sites of the +42 mRNA with in vitro CLIP. (*A*) Read coverage obtained by deep sequencing of 30S- or S1-protected *tisB* mRNA fragments. The footprints near the 5′ end, at the standby site, as well as upstream of and within the ORF are highlighted with double-head arrows (purple, blue, red, and black, respectively). (*B*) Secondary structure of the +42 *tisB* mRNA with the standby site highlighted (blue), RBS (green), and the *tisB* ORF (black), and S1 and 30S footprint coverage (from *A*) are indicated with double-head arrows (same color code).

30S-dependent reads or in a different pattern. We can tentatively exclude that the 30S footprints stem from free S1 after dissociation from the ribosome, since numerous reads from the 30S fraction, as expected, mapped to 16S rRNA (~150,000) (*SI Appendix*, Fig. S5).

A Secondary Structure Element at the 5′-End of +42 mRNA Is Required for Functional Standby. As proposed (19), a standby site requires a single-stranded sequence for 30S binding. The standby-competent +42 *tisB* mRNA indeed contains a ~15-nt-long ssRNA stretch with a fairly unstable upstream segment, which is absent in the 2 inactive +1 and +106 mRNAs (16). This unstructured region (light blue line; Fig. 4) showed many S1- and 30S-CLIP reads, and thus matched expectations. However, the reads mapping to the immediate 5′end of the mRNA were unanticipated, and suggested a so-far-overlooked element as part of the standby site (positions +42 to +69; Fig. 4*B*). To define the minimal functional standby site, successively 5′-truncated mRNAs were generated (Fig. 5*A*). The +62 and +66 *tisB* mRNAs are devoid of shorter hairpin elements upstream of the ss region. The +73 and +87 variants have extended ssRNA 5′ regions, whereas the +93 mRNA carries only the single-stranded standby sequence (Fig. 4*A* and *SI Appendix*, Fig. S6). As before, 30S-IC formation on +42 *tisB* mRNA generated a strong 30S/ $tRNA^{fMet}$-dependent RT stop at position +15. In contrast, none of the truncated mRNAs gave significant toeprint signals (Fig. 5*B*). When the same mRNAs were tested for TisB translation, 2 distinct TisB bands were observed for +42 *tisB* mRNA, as previously reported (16). All truncations decreased translation to background levels, and only the +93 mRNA gave a weak band (Fig. 5*C*). Thus, both toeprinting and in vitro translation results indicate that a structure element at the 5′ end of +42 *tisB* mRNA is functionally required for standby and contributes significantly to the translation efficiency of *tisB* mRNA.

The impairment in TisB translation due to 5′ truncations may reflect poor binding of S1 and, by extension, of the 30S subunit. To test this, we used fluorescence anisotropy on preformed S1 or 30S/5′-end FAM-labeled +42 *tisB* mRNA complexes challenged with a 50-fold molar excess of the truncated mRNA variants. Unlabeled +42 mRNA effectively displaced labeled mRNA from S1, whereas the truncated mRNAs had no significant effect (Fig. 5*D*), and the same result was obtained with 30S subunits (Fig. 5*E*). Thus, the truncated mRNAs are poor S1 and 30S binders.

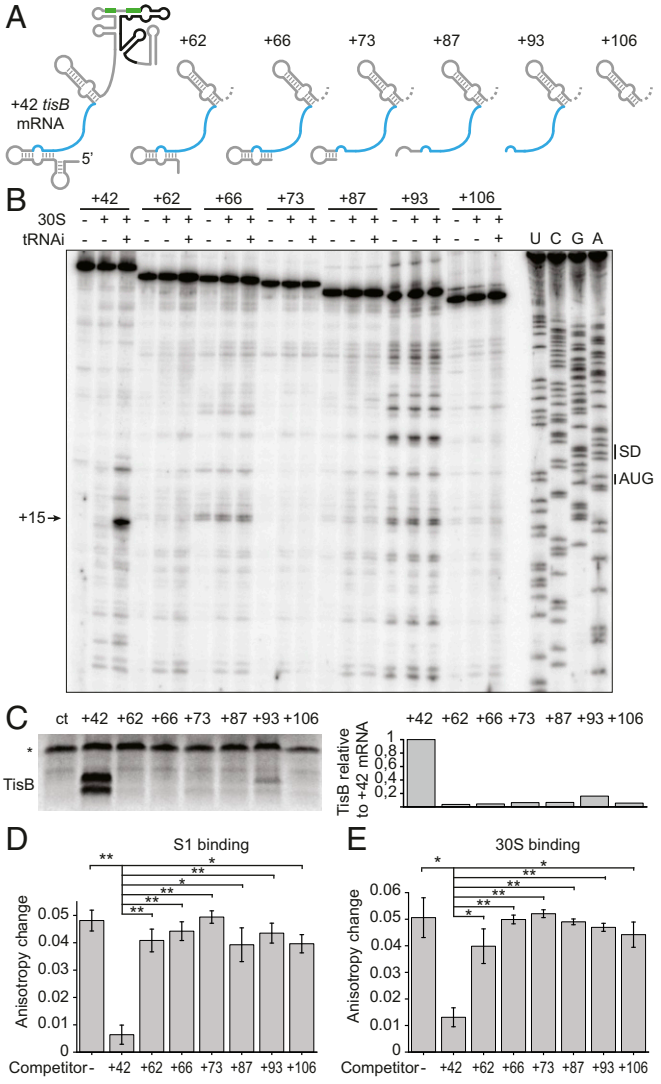

Fig. 5. A 5′-structural element is required for functional standby and *tisB* mRNA translation. (*A*) Schematics of the truncated *tisB* mRNAs. 5′UTR (gray), standby site (blue), ORF (black), and RBS (green). (*B*) Toeprint assay on the mRNAs as indicated, incubated alone, with 30S, or 30S+$tRNA^{fMet}$. The toeprint signal (+15 nt) is indicated, as are AUG and SD positions. (*C*, *Left*) In vitro translation of +42 *tisB* mRNA variants in the presence of S^{35}-Met. Lane "ct": no mRNA added; asterisk: unspecific label transfer to protein in the extract. See *SI Appendix, SI Materials and Methods*. (*C*, *Right*) Quantitation of band intensities from the gel. The intensity of TisB (+42 mRNA) was set to unity. (*D*) Competition experiments using 5′-end FAM-labeled +42 *tisB* mRNA (10 nM) incubated with 80 nM of S1 in the presence or absence of a 50-fold molar excess of the unlabeled mRNAs indicated. (*E*) Same set-up as in *D*, but with 30S (150 nM) replacing S1. Anisotropy change calculated from triplicates. **T*-test *P* values < 0.05; ***P* value < 0.005.

The importance of the 5′ stem-loop is further emphasized by the effect of a stem-breaker mutation, which abolishes 30S subunit binding and toeprint formation (*SI Appendix*, Figs. S1 *A* and *B* and S8). Moreover, 30S ribosomes bind to an RNA consisting only of the 5′-stem-loop and single-stranded region (*SI Appendix*, Fig. S1*A*). In conclusion, the functional *tisB* mRNA standby site consists of both the previously proposed ssRNA sequence and a 5′ end structure element.

Discussion

In this study, we define the anatomy of the natural standby site in the 5′UTR of *tisB* mRNA. Previous work identified the single-stranded region to which IstR-1 base pairs as a standby site (Fig. 1*A*) (16, 22, 31). Here, we provide evidence for direct $tRNA^{fMet}$-independent interaction of the 30S subunit to this sequence, based on fluorescence anisotropy: small subunits bind tightly to +42 mRNA (K_d 17 to 26 nM; Figs. 1*B* and 3*A* and *SI Appendix*, Fig. S4) and are displaced by IstR-1 and unlabeled +42 mRNA, but not by the standby-deficient +106 mRNA (Figs. 1 *B* and *C* and 3 *B* and *D*). Ribosomal protein S1 is required; standby-dependent toeprinting and translation are impaired in the absence of S1, but restored on readdition (Fig. 2 *A* and *B*). S1 anchors the 30S subunit to the standby site, as 30SΔS1 ribosomes do not bind +42 mRNA (Fig. 2*C*), S1 alone binds tightly to the standby mRNA with characteristics comparable to 30S subunits (Fig. 3), and the read profiles of cross-linked S1 and 30S subunits are almost identical (Fig. 4*A*).

The CLIP experiment gave additional information. As expected, many S1- and 30S-dependent reads mapped to the single-stranded region (+85 to +111; Fig. 4*B*), but surprisingly, also to the immediate 5′-end of +42 mRNA (+42 to +69; Fig. 4*B*). This suggested an element as part of the binding site that, based on chemical and enzymatic probing, is a 5′-stem-loop (*SI Appendix*, Figs. S6 and S7); its mutational disruption prevented *tisB* toeprinting (*SI Appendix*, Fig. S8). Indeed, all 5′-truncated +42 mRNAs (Fig. 5*A*) failed to support standby-dependent initiation and TisB translation (Fig. 5 *B* and *C*), and were poor competitors for S1 and 30S binding to +42 mRNA (Fig. 5 *D* and *E*), as was the 5′-stem-loop breaker mutant mRNA (*SI Appendix*, Fig. S1*A*).

The standby dependence on S1 is intriguing and tentatively suggests how standby, in the *tisB* case, may overcome structural sequestration at a great distance. Binding of S1 to the single-stranded region, alone or in the context of the 30S subunit, may entail successive unfolding steps, in line with biochemical studies (17, 30). This may explain the 2 clusters of CLIP reads closer to, and within, the *tisB* ORF (Fig. 4*A*), which are dependent on prior S1/30S binding to the single-stranded region and the 5′-terminal element, based on the combined results presented here (Figs. 1 *B* and *C*, 2*C*, 3 *B* and *D*, and 5 *D* and *E*). Directional unwinding also fits the result that a DNA oligo base-paired downstream of the standby site acts as a roadblock for *tisB* RBS access (16), even though 30S and S1 standby binding still occurs (*SI Appendix*, Fig. S1*A*).

An elegant study showed recently how a standby site immediately upstream of an accessible RBS in *E. coli lpp* mRNA can promote very high TE. Standby, in this case, kinetically boosts translation rates since the recruited 30S subunit is ready to initiate as soon as the first 70S ribosome has departed from the RBS (32). Also here, ribosomal protein S1 (and S2), is important for standby-dependent polysome formation, whereas essential structure elements appear not to be involved. It is striking that standby can solve problems on opposite ends of a TE scale. In the *tisB* case, standby at a great distance enables translation from an otherwise inaccessible RBS, whereas in the *lpp* case, it increases initiation rates from an already accessible RBS.

It is worth pointing out that standby definitions have shifted somewhat since the MS2-based mechanism was proposed. For example, in a biophysical model (33, 34), standby binding involving the combined single-stranded surface area around a translation start site contributes to a combined ΔG-value (of SD-anti-SD, $tRNA^{fMet}$-AUG, SD-AUG spacing, and standby) that correlates with initiation probability. Although these predictions are generally powerful, they fail to account for standby effects in *tisB*. When running active and inactive *tisB* mRNA variants in the RBS calculator algorithm (https://salislab.net/software/reverse) (33, 34), the predicted expression of the *tisB* ORF was both very low and also identical for all mRNA tested (*SI Appendix*, Table S3). This likely reflects that standby from a long distance cannot be handled by the algorithm or that, in our case, a ΔG-based model is not adequate.

The 30S platform has also been described as a universal standby site, able to bind structured mRNAs. In contrast to the *tisB* mRNA, the anchoring of *rpsO* mRNA on the 30S platform requires the SD/anti-SD interaction (18), which again is dependent on S1 (17, 18). Other standby models are clearly conceivable. 30S binding to a structurally complex mRNA operator could facilitate a folding rearrangement to permit access to the sequestered RBS. Although our data do not exclude such a model, there is at this point little support. For example, 30S subunits do not bind the *tisB* mRNA 3′-domain, whereas a 5′ mRNA segment containing only the 5′-stem-loop and the downstream ss region does (*SI Appendix*, Fig. S1*A*). Also, congruent translation and toeprinting results suggest that, since the toeprinting oligo base pairs toward the end of the coding region (e.g., Figs. 2 and 5), structural changes are unlikely to account for standby effects.

Most standby models involve single-stranded regions that are bound sequence-nonspecifically by 30S subunits. Single-stranded 5′-tails can act as a binding platform for 30S to bind in immediate vicinity of stable hairpins, and can act as standby sites to promote a high translation rate of mRNAs in which an RBS is sequestered (20, 21). Based on the data presented, the standby site in +42 *tisB* mRNA suggests a more complex picture. Clearly, the single-stranded standby region is required for binding of S1 and S1-containing ribosomes, and is the site at which IstR-1 blocks binding and thus standby-dependent TisB translation. The additional requirement for a structure element (Figs. 4 and 5 and *SI Appendix*, Figs. S7 and S8) suggests 2 ways for contributing to standby. First, the additional interaction between this element and S1 or 30S subunits increases affinity (e.g., Figs. 4 and 5 *D* and *E*). Of note, S1 avidly binds RNA pseudoknots (35). Chemical structure mapping, however, could not conclusively distinguish between a 5′-stem-loop (*SI Appendix*, Fig. S7) and a pseudoknot structure. Second, a 5′ structure could serve as a bookend to constrain the proper positioning of the ribosome on standby (see below).

A shared feature for standby binding, irrespective of the different consequences discussed here, is sequence-independent binding of a free 30S to an unstructured RNA region (16, 19–21, 32, 33) Clearly, this also applies to *tisB*, but 2 aspects differ: the great distance at which the effect is exerted and the requirement of a 5′ structure for functional standby (Fig. 5). Notably, a structure element may also be required for standby in another TA system, *zorO*/*orzO*, with characteristics reminiscent of *tisB*/*istR-1* (36). This unexpected result may be related to a recent observation: a short hairpin in the coding sequence of *fepA* mRNA promotes translation initiation by constraining lateral sliding of the 30S subunit, thus positioning it effectively at the RBS (37). This might indicate that structures either upstream or downstream of a 30S binding site (standby or bona fide RBS) are a common solution to increase the half-life of 30S–mRNA complexes.

At this point, it is unclear whether the standby mechanism in *tisB* is a rare or widespread case. Structures at/near RBSs have been observed, which may be required for mRNA stabilization or as binding sites for metabolites, sRNAs, or regulatory proteins. In such cases, standby might be a mechanism to obtain appropriate translation rates.

Materials and Methods

Strains. Strains and primers used in this study are listed in *SI Appendix*, Table S1. A chromosomal *rpsA-3xFLAG* gene was generated by scarless mutagenesis (38).

BIOCHEMISTRY

Ribosome Preparation and Protein S1 Purification. Ribosome preparation, S1 depletion (17), and purification of S1 was performed as in *SI Appendix, SI Materials and Methods*.

Fluorescence Anisotropy Measurements. Five or 10 nM (final concentration) of fluorescein-labeled mRNA were denatured for 2 min at 90 °C, followed by 1 min on ice, and then renatured in native buffer 1× (50 mM Tris·HCl at pH 7.5, 100 mM K-acetate, 10 mM DTE, and 10 mM $MgCl_2$) at 37 °C for 15 min. 30S or purified S1 were added to the reaction mix with or without competitor RNAs (50-fold molar excess of unlabeled mRNA over labeled RNA). Complexes were allowed to form for 20 min at 37 °C. Fluorescein was excited with polarized light (λ_{ex} = 485 nm) and polarized parallel, and orthogonal emission (λ_{em} = 535 nm) was recorded using a Tecan SPARK 10M.

In Vitro Transcription of RNA and FAM Adaptor Ligation. RNAs were in vitro transcribed (Megascript kit; Life Technologies, #AM1330) from PCR-generated DNA templates using hot start Phusion (see *SI Appendix*, Table S2 for the primers). RNAs were purified by denaturing PAGE, followed by phenol extraction and ethanol precipitation. FAM groups were introduced at either the 5′- or the 3′-ends of mRNAs, as described in *SI Appendix, SI Materials and Methods*.

Toeprint Assays. Toeprint assays were performed essentially as in ref. 16, with more details given in *SI Appendix, SI Materials and Methods*.

In Vitro Translation Assay and Protein Detection. Translation was assayed in the PURExpress In Vitro Protein Synthesis system (E6800S, New England BioLabs) in 10-μL reaction volumes. Detection of FLAG-tagged TisB (in Fig. 2*B*) or by radioactive labeling (in Fig. 5*C*) is described in *SI Appendix, SI Materials and Methods*. To test 70SΔS1 functionality, the PURExpress ΔRibosome Kit (E3313S, New England BioLabs) was used instead and supplemented with purified 30S and 50S subunits.

In Vitro CLIP. CLIP experiment were based on the ability to pull down 3xFLAG protein using Anti-FLAG magnetic beads (Sigma, A2220). In all experiments, either S1-3xFLAG or 30S containing S1-3xFLAG were used. Next, 15 pmol purified +42 mRNA was denatured for 1 min at 90 °C, placed on ice for 2 min, and renatured in native buffer (50 mM Tris·HCl at pH 7.5, 100 mM K-acetate, 10 mM DTE, 10 mM $MgCl_2$) at 37 °C for 15 min. Then, 10 pmol of S1 or 30S subunits was added, followed by 15 min incubation at 37 °C. RNA–protein complexes were cross-linked by UV at 254 nm (UVC500 cross-linker; Amersham, 250 mJ/cm^2). RNA footprints were generated on the beads with benzonase (0.5 U/μL) for 10 min at 37 °C. Proteins were digested with proteinase K (Thermo Fisher Scientific, EK0031) and labeled RNA footprints (25 to 50 nt) gel-purified. Eluted RNAs were converted into cDNA, using the CATS RNA-Seq kit v2 (diagenode, C05010045), and sequenced on an Illumina Miseq device.

ACKNOWLEDGMENTS. We thank S. Sanyal for $tRNA^{fMet}$ and purified 50S subunits, A. Sabantsev for help with initial fluorescence anisotropy experiments, D. Huseby for RNA sequencing help, and C. Ducani in DMS experiments. Plasmid pET S1-His6 was a generous gift from S. Marzi. We are grateful to M. Ehrenberg, P. Romby, and S. Marzi for critical reading of the manuscript, and E. Westhof for advice. We acknowledge support from The Swedish Research Council (E.G.H.W.), the European Research Council (S.D.), and the Knut and Alice Wallenberg Foundation (S.D.).

1. G.-W. Li, D. Burkhardt, C. Gross, J. S. Weissman, Quantifying absolute protein synthesis rates reveals principles underlying allocation of cellular resources. *Cell* **157**, 624–635 (2014).
2. P. Milón, M. V. Rodnina, Kinetic control of translation initiation in bacteria. *Crit. Rev. Biochem. Mol. Biol.* **47**, 334–348 (2012).
3. C. O. Gualerzi, C. L. Pon, Initiation of mRNA translation in bacteria: Structural and dynamic aspects. *Cell. Mol. Life Sci.* **72**, 4341–4367 (2015).
4. A. Hüttenhofer, H. F. Noller, Footprinting mRNA-ribosome complexes with chemical probes. *EMBO J.* **13**, 3892–3901 (1994).
5. M. M. Meyer, The role of mRNA structure in bacterial translational regulation. *Wiley Interdiscip. Rev. RNA* **8**, e1370 (2017).
6. M. V. Rodnina, Translation in Prokaryotes. *Cold Spring Harb. Perspect. Biol.* **10**, a032664 (2018).
7. A. Simonetti *et al.*, A structural view of translation initiation in bacteria. *Cell. Mol. Life Sci.* **66**, 423–436 (2009).
8. J. Shine, L. Dalgarno, The 3′-terminal sequence of Escherichia coli 16S ribosomal RNA: Complementarity to nonsense triplets and ribosome binding sites. *Proc. Natl. Acad. Sci. U.S.A.* **71**, 1342–1346 (1974).
9. J. A. Steitz, K. Jakes, How ribosomes select initiator regions in mRNA: Base pair formation between the 3′ terminus of 16S rRNA and the mRNA during initiation of protein synthesis in Escherichia coli. *Proc. Natl. Acad. Sci. U.S.A.* **72**, 4734–4738 (1975).
10. A. Goyal, R. Belardinelli, C. Maracci, P. Milón, M. V. Rodnina, Directional transition from initiation to elongation in bacterial translation. *Nucleic Acids Res.* **43**, 10700–10712 (2015).
11. C. Del Campo, A. Bartholomäus, I. Fedyunin, Z. Ignatova, Secondary structure across the bacterial transcriptome reveals versatile roles in mRNA regulation and function. *PLoS Genet.* **11**, e1005613 (2015).
12. D. Voges, M. Watzele, C. Nemetz, S. Wizemann, B. Buchberger, Analyzing and enhancing mRNA translational efficiency in an Escherichia coli in vitro expression system. *Biochem. Biophys. Res. Commun.* **318**, 601–614 (2004).
13. G. Kudla, A. W. Murray, D. Tollervey, J. B. Plotkin, Coding-sequence determinants of gene expression in Escherichia coli. *Science* **324**, 255–258 (2009).
14. A. Espah Borujeni *et al.*, Precise quantification of translation inhibition by mRNA structures that overlap with the ribosomal footprint in N-terminal coding sequences. *Nucleic Acids Res.* **45**, 5437–5448 (2017).
15. M. H. de Smit, J. van Duin, Secondary structure of the ribosome binding site determines translational efficiency: A quantitative analysis. *Proc. Natl. Acad. Sci. U.S.A.* **87**, 7668–7672 (1990).
16. F. Darfeuille, C. Unoson, J. Vogel, E. G. H. Wagner, An antisense RNA inhibits translation by competing with standby ribosomes. *Mol. Cell* **26**, 381–392 (2007).
17. M. Duval *et al.*, Escherichia coli ribosomal protein S1 unfolds structured mRNAs onto the ribosome for active translation initiation. *PLoS Biol.* **11**, e1001731 (2013).
18. S. Marzi *et al.*, Structured mRNAs regulate translation initiation by binding to the platform of the ribosome. *Cell* **130**, 1019–1031 (2007).
19. M. H. de Smit, J. van Duin, Translational standby sites: How ribosomes may deal with the rapid folding kinetics of mRNA. *J. Mol. Biol.* **331**, 737–743 (2003).
20. S. M. Studer, S. Joseph, Unfolding of mRNA secondary structure by the bacterial translation initiation complex. *Mol. Cell* **22**, 105–115 (2006).
21. M. Sterk, C. Romilly, E. G. H. Wagner, Unstructured 5′-tails act through ribosome standby to override inhibitory structure at ribosome binding sites. *Nucleic Acids Res.* **46**, 4188–4199 (2018).
22. J. Vogel, L. Argaman, E. G. H. Wagner, S. Altuvia, The small RNA IstR inhibits synthesis of an SOS-induced toxic peptide. *Curr. Biol.* **14**, 2271–2276 (2004).
23. C. Unoson, E. G. H. Wagner, A small SOS-induced toxin is targeted against the inner membrane in Escherichia coli. *Mol. Microbiol.* **70**, 258–270 (2008).
24. B. A. Berghoff, M. Hoekzema, L. Aulbach, E. G. H. Wagner, Two regulatory RNA elements affect TisB-dependent depolarization and persister formation. *Mol. Microbiol.* **103**, 1020–1033 (2017).
25. J. Czworkowski, O. W. Odom, B. Hardesty, Fluorescence study of the topology of messenger RNA bound to the 30S ribosomal subunit of Escherichia coli. *Biochemistry* **30**, 4821–4830 (1991).
26. J. Sengupta, R. K. Agrawal, J. Frank, Visualization of protein S1 within the 30S ribosomal subunit and its interaction with messenger RNA. *Proc. Natl. Acad. Sci. U.S.A.* **98**, 11991–11996 (2001).
27. M. A. Sørensen, J. Fricke, S. Pedersen, Ribosomal protein S1 is required for translation of most, if not all, natural mRNAs in Escherichia coli in vivo11Edited by D. Draper. *J. Mol. Biol.* **280**, 561–569 (1998).
28. E. Hajnsdorf, I. V. Boni, Multiple activities of RNA-binding proteins S1 and Hfq. *Biochimie* **94**, 1544–1553 (2012).
29. I. V. Boni, D. M. Isaeva, M. L. Musychenko, N. V. Tzareva, Ribosome-messenger recognition: mRNA target sites for ribosomal protein S1. *Nucleic Acids Res.* **19**, 155–162 (1991).
30. X. Qu, L. Lancaster, H. F. Noller, C. Bustamante, I. Tinoco, Jr, Ribosomal protein S1 unwinds double-stranded RNA in multiple steps. *Proc. Natl. Acad. Sci. U.S.A.* **109**, 14458–14463 (2012).
31. E. G. H. Wagner, C. Unoson, The toxin-antitoxin system tisB-istR1: Expression, regulation, and biological role in persister phenotypes. *RNA Biol.* **9**, 1513–1519 (2012).
32. I. Andreeva, R. Belardinelli, M. V. Rodnina, Translation initiation in bacterial polysomes through ribosome loading on a standby site on a highly translated mRNA. *Proc. Natl. Acad. Sci. U.S.A.* **115**, 4411–4416 (2018).
33. A. Espah Borujeni, A. S. Channarasappa, H. M. Salis, Translation rate is controlled by coupled trade-offs between site accessibility, selective RNA unfolding and sliding at upstream standby sites. *Nucleic Acids Res.* **42**, 2646–2659 (2014).
34. H. M. Salis, E. A. Mirsky, C. A. Voigt, Automated design of synthetic ribosome binding sites to control protein expression. *Nat. Biotechnol.* **27**, 946–950 (2009).
35. S. Ringquist *et al.*, High-affinity RNA ligands to Escherichia coli ribosomes and ribosomal protein S1: Comparison of natural and unnatural binding sites. *Biochemistry* **34**, 3640–3648 (1995).
36. J. Wen, J. R. Harp, E. M. Fozo, The 5′ UTR of the type I toxin ZorO can both inhibit and enhance translation. *Nucleic Acids Res.* **45**, 4006–4020 (2017).
37. J. Jagodnik, C. Chiaruttini, M. Guillier, Stem-loop structures within mRNA coding sequences activate translation initiation and mediate control by small regulatory RNAs. *Mol. Cell* **68**, 158–170.e3 (2017).
38. J. Näsvall, A. Knöppel, D. I. Andersson, Duplication-insertion recombineering: A fast and scar-free method for efficient transfer of multiple mutations in bacteria. *Nucleic Acids Res.* **45**, e33 (2017).